Parameters that Specify the Timing of Cytokinesis

Charles B. Shuster*‡ and David R. Burgess§

*Department of Biological Sciences, University of Pittsburgh, Pittsburgh, Pennsylvania 15260; ‡Mount Desert Island Biological Laboratory, Salisbury, Maine 04672; and §Department of Biology, Boston College, Chestnut Hill, Massachusetts 02467

Abstract. One model for the timing of cytokinesis is based on findings that $p34^{cdc2}$ can phosphorylate myosin regulatory light chain (LC20) on inhibitory sites (serines 1 and 2) in vitro (Satterwhite, L.L., M.H. Lohka, K.L. Wilson, T.Y. Scherson, L.J. Cisek, J.L. Corden, and T.D. Pollard. 1992. *J. Cell Biol.* 118:595–605), and this inhibition is proposed to delay cytokinesis until $p34^{cdc2}$ activity falls at anaphase. We have characterized previously several kinase activities associated with the isolated cortical cytoskeleton of dividing sea urchin embryos (Walker, G.R., C.B. Shuster, and D.R. Burgess. 1997. *J. Cell Sci.* 110:1373–1386). Among these kinases and substrates is $p34^{cdc2}$ and LC20. In comparison with whole cell activity, cortical H1 kinase activity is delayed, with maximum levels in cortices prepared from late anaphase/telophase embryos. To determine whether cortical-associated $p34^{cdc2}$ influences cortical myosin II activity during cytokinesis, we labeled eggs in vivo with [^{32}P]orthophosphate, prepared cortices, and mapped LC20 phosphorylation through the first cell division. We found no evidence of serine 1,2 phosphorylation at any time during mitosis on LC20 from cortically associated myosin. Instead, we observed a sharp rise in serine 19 phosphorylation during anaphase and telophase, consistent with an activating phosphorylation by myosin light chain kinase. However, serine 1,2 phosphorylation was detected on light chains from detergent-soluble myosin II. Furthermore, cells arrested in mitosis by microinjection of nondegradable cyclin B could be induced to form cleavage furrows if the spindle poles were physically placed in close proximity to the cortex. These results suggest that factors independent of myosin II inactivation, such as the delivery of the cleavage stimulus to the cortex, determine the timing of cytokinesis.

Key words: cytokinesis • $p34^{cdc2}$ • myosin II • sea urchin • phosphorylation

THE assembly of an actomyosin-based contractile ring at the conclusion of mitosis has long been a topic of great interest, but the regulation of cytokinesis remains a poorly understood process in animal cells. Although the basic structural elements of the contractile ring have been recognized for some time (Schroeder, 1968, 1972; Fujiwara and Pollard, 1976), recent genetic analyses in yeast and in higher eukaryotes have identified additional components that may play structural or organizational roles in the assembly of the actomyosin ring (Glotzer, 1997; Field et al., 1999), and have reexamined the role of myosin II–based contractility in cleavage furrow formation (Neujahr et al., 1997; Zang et al., 1997). Yet despite these advances, consensus on how chromosome segregation and cytoplasmic partitioning are regulated in space and time remains elusive.

Micromanipulation studies in echinoderm embryos as well as tissue culture cells indicate that the position of the cleavage furrow is specified by microtubules of the mitotic apparatus (for reviews see Rappaport, 1996, and Glotzer, 1997). Yet the exact mechanism by which microtubules impart spatial information to the cortex or the population of microtubules that participate in this process remains controversial. In spherical echinoderm eggs, astral microtubules specify the equatorial position of the cleavage plane, since furrows may be induced wherever there are overlapping aster centers regardless of whether there is a spindle midzone present (Rappaport, 1961). The influence of the spindle midzone may predominate in tissue culture cells, where study of heterokaryons as well as physical blocks placed between the cortex and the midzone implicate the spindle midzone in specifying the position of the contractile ring (Cao and Wang, 1995; Wheatley and Wang, 1996). In contrast, similar studies of heterokaryons and other cells with multiple spindles have reached conclusions that agree with those drawn from studies of echinoderm eggs (Rieder et al., 1997; Sanger et al., 1998). However, recent reports (Hamaguchi, 1998; Savoian et al., 1999) may ultimately reconcile these disparate results by

Dr. Shuster's present address is Higgins Hall, Department of Biology, Boston College, Chestnut Hill, MA 02467.

Address correspondence to David R. Burgess, Department of Biology, Boston College, 432 Higgins Hall, Chestnut Hill, MA 02467. Tel.: (617) 552-1606. Fax: (617) 552-2011. E-mail: david.burgess@bc.edu

invoking microtubule density (as opposed to a distinct population of microtubules) as the ultimate determinant of furrow formation.

Another outstanding question regards how the timing of cytokinesis is coordinated with the processes of karyokinesis, or chromosome segregation. The entry into mitosis is driven by the cyclic activation of the cyclin-dependent kinase $p34^{cdc2}$ (Nurse, 1990). Directly or indirectly, $p34^{cdc2}$ orchestrates the remodeling of the actin and intermediate filament cytoskeletons and the acceleration of microtubule dynamics, as well as chromatin condensation and nuclear envelope breakdown. Normally, cleavage furrows are not observed until $p34^{cdc2}$ activity falls after anaphase onset, at which time microtubules emanating from the spindle poles contact the cortex and induce the formation of a cleavage furrow. Indeed, cells injected with nondegradable forms of cyclin B are capable of undergoing anaphase-like spindle movements and chromosome segregation, but fail to divide (Wheatley et al., 1997; Hinchcliffe et al., 1998). It has been proposed that $p34^{cdc2}$ acts as the timer for cytokinesis by regulating myosin II activity (Satterwhite and Pollard, 1992). This model is based on in vitro experiments in which $p34^{cdc2}$ phosphorylates myosin II regulatory light chain (LC20) (Satterwhite et al., 1992) on sites shown previously to inhibit myosin ATPase activity when phosphorylated by protein kinase C (PKC)[1] (Nishikawa et al., 1984; Bengur, 1987; Ikebe and Reardon, 1990). Indeed, in vivo analyses of LC20 phosphorylation demonstrate that serine 1,2 phosphorylation is detected in cells arrested in mitosis with microtubule-destabilizing reagents, whereas serine 19 phosphorylation predominates when the arrest is lifted and the cells proceed through cytokinesis (Yamakita et al., 1994). These results are consistent with observations using either biosensors or phosphoepitope antibodies specific for serine 19, where an accumulation of serine 19 phosphorylated light chains can be detected in cleavage furrows (DeBiasio et al., 1996; Matsumura et al., 1998; Murata-Hori et al., 1998). Taken together, these data point toward a mechanism by which myosin motor activity is held in check until anaphase onset, at which time the cortex receives positional information from the mitotic apparatus, and a furrow may be established.

However, maturation promoting factor (MPF) modulates the activities of a vast array of structural and regulatory elements, and circumstantial evidence suggests that actomyosin-based contractility may not be tightly coupled to the cyclic activation and destruction of MPF activity. Alterations of the geometrical relationship between the mitotic apparatus and the cell surface of sand dollar eggs reveal that the mitotic apparatus is capable of inducing furrows over a much wider window of time (a period spanning 56% of the cell cycle) than what might be predicted from a cdc2-based cortical inactivation model, with furrows induced both earlier and later than the normal time of induction (Rappaport, 1975, 1985; Rappaport and Rappaport, 1993). In addition, during the syncytial blastoderm stage of *Drosophila* embryogenesis, transient invaginations termed pseudo or metaphase furrows ingress between adjacent spindles only to regress during anaphase (Miller and Kiehart, 1995). These furrows contain both actin and myosin, and do not progress to completion until the 14th division. In contrast to normal cleavage furrows, these actomyosin-based structures form precisely during the time that MPF activity is highest in the embryo. Together, these observations suggest that contractile ring assembly may not be limited to a narrow window of time following anaphase onset and resumption of the next cell cycle, as might be predicted by the Satterwhite and Pollard (1992) model.

We have employed echinoderm embryos as a model system to biochemically dissect the spatial and temporal regulation of cytokinesis. Sea urchin and sand dollar embryos not only afford the high degree of synchrony required for such analyses, but also benefit from the extensive lines of experimentation regarding the relationship between the mitotic apparatus and the establishment of the cleavage furrow. Toward these ends we have developed previously a detergent-extracted preparation of the sea urchin cortical cytoskeleton that retains the morphological, biochemical, and functional characteristics of the intact zygote (Walker et al., 1994). In addition, we have also characterized the presence of several protein kinases (and their substrates) that are present and active within the cortical cytoskeleton whose activities peak during cleavage (Walker et al., 1996, 1997). Identified among these kinases by histone H1 kinase activity and Western blotting is $p34^{cdc2}$. Interestingly, the H1 kinase activity peaked in cortices prepared from telophase blastomeres. Given that whole cell $p34^{cdc2}$ activity typically peaks when cells are in metaphase, and taking into account current hypotheses proposed for the timing of cytokinesis, we have revisited the role that $p34^{cdc2}$ plays in the timing of cytokinesis, particularly with regard to its role in myosin regulation. Biochemical analyses of myosin II regulatory light chain phosphorylation, in combination with an in vivo assessment of cortical responsiveness to stimulatory signals from the spindle, indicate that $p34^{cdc2}$ specifies the timing of cytokinesis through mechanisms independent of myosin II negative regulation.

Materials and Methods

Embryo Culture

The sea urchin *Lytechinus pictus* was obtained from Marinus, Inc. and the sand dollar *Echinarachnius parma* was used on site at the Mount Desert Island Biological Laboratory. Gametes were obtained by intracoelemic injection of 0.5 M KCl, and after fertilization the fertilization envelopes were removed either by passage through Nitex membranes or by treatment with 1 M glycine. Zygotes were then cultured in filtered sea water at 16–17°C.

Preparation of Whole Cell and Cytoskeletal Fractions for Histone H1 Kinase Assays

Cortical cytoskeletons and whole cell extracts were prepared essentially as described in Walker et al. (1997). In brief, at time points before or following fertilization, 100 μl of eggs was washed once in isolation buffer (20 mM Pipes, pH 7.3, 5 mM $MgCl_2$, 5 mM EGTA, 1 M glycerol, 5 mM sodium vanadate, 25 mM NaF) supplemented with 10 μg/ml soybean trypsin inhibitor, benzamidine, leupeptin, α2-macroglobulin, aprotinin, and 1 mM PMSF. Half of the washed cells were resuspended, vortexed, and snap frozen in 20 vol of EB (80 mM β-glycerophosphate, 10 mM $MgCl_2$, 10 mM

1. *Abbreviations used in this paper:* MAP, mitogen-activated protein; MLCK, myosin light chain kinase; MPF, maturation promoting factor; PKC, protein kinase C.

EGTA plus protease inhibitors), and the other half were lysed for 10 min on ice in 20 vol of isolation buffer containing 0.5% NP-40 and protease inhibitors. The detergent-extracted embryos were then homogenized in a loose-fitting dounce homogenizer, and washed three times by pelleting and resuspension in isolation buffer minus detergent. The washed cortices were then resuspended in 50 μl of isolation buffer and snap frozen in liquid nitrogen.

To assay for $p34^{cdc2}$ activity, whole cell and cortical fractions were thawed on ice, diluted fourfold in EB, and a fraction was set aside to determine the protein concentration. 10 μl of the diluted fraction was then mixed with 10 μl of a reaction mix containing 1 mg/ml histone H1, 200 μM [γ-^{32}P]ATP (2 Ci/mmol), 20 μM H-7, and the mixture was incubated at 20°C for 20 min. The reactions were stopped by addition of boiling 2× SDS-PAGE sample buffer. Samples were resolved by SDS-PAGE, and following Coomassie blue staining and drying, phosphorylation was analyzed by autoradiography and scintillation counting. Histone phosphorylation was normalized to the extract protein concentrations as measured by BCA assay (Biorad). To test cortical H1 kinase for sensitivity to kinase inhibitors, cortices prepared from dividing zygotes were diluted into EB and assayed for H1 kinase activity in the presence or absence of 5 μM roscovitine, 10 μM olomoucine, 10 μM isoolomoucine, 20 μM H-7, 10 μM ML-9, or 10 μM genistein.

Metabolic Labeling and Myosin Light Chain Phosphopeptide Mapping

1 ml packed eggs was incubated in the presence of 5 mCi [^{32}P]orthophosphoric acid in 4 ml phosphate-free sea water for 60 min at 15°C. Eggs were then washed free of label, and fertilized. In some experiments, eggs were fertilized and cultured in the presence of ^{32}P up until nuclear envelope breakdown, at which time eggs were washed free of label. Incubating eggs before or after fertilization had no effect on the patterns of phosphate incorporation into myosin regulatory light chain. At time points through the first mitosis, cortical cytoskeletons were prepared as described above. In some experiments, the detergent soluble fraction was clarified at 14,000 *g* and with 10 μl of either normal rabbit serum or rabbit anti–egg myosin antibodies for 2 h at 4°C. The immune complexes were harvested with protein G agarose (Amersham Pharmacia Biotech) and washed three times in TBS containing 1% Triton X-100, 25 mM NaF, and 5 mM sodium vanadate. The resultant cortices or immunoprecipitates were resolved by SDS-PAGE, transferred to Immobilon P membranes, stained with Coomassie blue R-250, and phosphorylated polypeptides were visualized by autoradiography. Regulatory light chains were identified as bands comigrating with purified light chains or light chains immunoprecipitated from sea urchin whole cell extracts with myosin heavy chain antibodies. Light chains were excised from the immobilon membranes, and nonspecific sites were blocked in 0.5% polyvinylpyrridone in 100 mM acetic acid for 1 h at 37°C. Light chains were then digested overnight with 160 μg/ml TPCK-trypsin in 50 mM ammonium bicarbonate, pH 8.0, at 37°C. The peptide digests were then subjected to four rounds of lyophilization and resuspension in water to remove the bicarbonate. Samples were then resuspended in pH 1.9 buffer (2.2% formic acid, 7.8% acetic acid) and spotted onto a cellulose TLC plate. Samples were subjected to electrophoresis for 60 min at 1,000 V using a Hunter high voltage electrophoresis system (C.B.S. Scientific Co.), and then subjected to liquid chromatography in a second dimension in phosphochromatography buffer (37.5% *n*-butanol, 25% pyridine, 7.5% acetic acid) for 5 h. The plates were then dried and the peptide digests visualized by autoradiography. Tryptic peptide assignments were based on Satterwhite et al. (1992). Purified brush border (provided by Dr. Karl Fath, University of Pittsburgh, Pittsburgh, PA) or sea urchin egg myosin II (Yabkowitz and Burgess, 1987) were phosphorylated in vitro with either gizzard myosin light chain kinase (MLCK) (provided by Dr. R. Adelstein, National Institutes of Health, Bethesda, MD) or the catalytic fragment of PKC (Calbiochem) according to Satterwhite et al. (1992), and subjected to peptide digestion and phosphopeptide analysis. When PKC- or MLCK-phosphorylated brush border and sea urchin egg myosin light chain were mixed and subjected to phosphopeptide analysis, the resultant maps were superimposable. These digests served as standards to identify phosphopeptides from in vivo–phosphorylated samples.

In Vitro Phosphorylation

To determine whether $p34^{cdc2}$ phosphorylation of myosin light chain affects the association of myosin II with the cortical cytoskeleton, cortical cytoskeletons were prepared from interphase zygotes (~30 min after fertilization), when cortical kinase activity was low (Walker et al., 1997). 30 μl suspensions of cortices were incubated either alone or in the presence of 10^{-8} M PKC or $p34^{cdc2}$–cyclin B complex and 200 μM [γ-^{32}P]ATP (2 Ci/mmol) for 25 min at 20°C. The reactions were clarified for 5 min at 14,000 *g*. The supernatants were removed and the cortices resuspended in a matching volume of isolation buffer. SDS-PAGE sample buffer was added to both fractions, and after boiling, equal volumes were loaded onto 12% SDS-PAGE gels, transferred to Immobilon membranes, and light chains were detected by autoradiography and immunoblotting with rabbit anti–egg myosin antiserum that recognizes both heavy and light chains.

Microinjection and Micromanipulation

To arrest cells in mitosis, a truncated form of *Arbacia punctulata* cyclin B (Δ90 cyclin) was expressed in bacteria and purified as described previously (Glotzer et al., 1991). As an additional purification step, the enriched Δ90 cyclin fraction (~80% pure) was clarified and applied to a Superose 12 FPLC column, and peak fractions were >90% homogenous. The purified cyclin was dialyzed against injection buffer (10 mM Hepes, 100 mM potassium aspartate, pH 7.2), and concentrated to ~2 mg/ml with Microcon™ concentrators (Amicon). The activity of the recombinant protein was assessed in vitro before microinjection by testing the ability of Δ90 cyclin to arrest *Xenopus* cycling extracts in mitosis.

For microinjection of Δ90 cyclin, *E. parma* embryos were fertilized, stripped of their fertilization envelopes and hyaline layers, and cultured through the first division at 16°C. Two cell embryos were then held in place with a holding pipette, and one blastomere was injected with injection buffer alone or injection buffer containing Δ90 cyclin; injected blastomeres were then marked with a small volume of Wesson oil. The uninjected blastomere served as a time control. Embryos were then scored for cleavage. Injection volumes varied between 0.5 and 4%, resulting in an intracellular concentration of ~1 μM Δ90 cyclin. To confirm that Δ90-injected blastomeres were arrested in mitosis, and because sand dollar embryo chromosomes are difficult to discern by standard light microscopy, injected blastomeres were cultured in injection chambers (Kiehart, 1982) in the presence of 1 μg/ml Hoescht No. 33342, and chromatin condensation was observed by fluorescence microscopy. To assess the contractile state of the cortex in Δ90-arrested cells, blastomeres were injected and incubated until prophase spindles were visible in the uninjected blastomeres. A needle was then lowered onto the injected cell parallel to the plane of the coverslip, bisecting the cell and pressing the spindle poles towards the cell surface. Another needle was placed adjacent to the injected blastomere to hold the embryo in place. An alternative method for altering the geometrical relationship between the spindle poles and the surface was to draw control or Δ90-injected blastomeres into a fire-polished pipette with an internal diameter between 40 and 65 μm. Bright field images were recorded on a Leitz diavert microscope with Tech pan film ASA 200, and figures were prepared using Adobe Photoshop® software.

Results

The Kinetics of Cytoskeletal and Whole Cell Histone H1 Kinase Activity Differ during Cell Division

Previous work in the laboratory (Walker et al., 1996, 1997) has characterized several protein kinases associated and active within the actin-based cortical cytoskeleton of dividing sea urchin blastomeres. Among these are the tyrosine kinases abl and fyn, a mitogen-activated protein (MAP) kinase, and as yet uncharacterized kinases of 42, 45, and 84 kD. A histone H1 kinase activity was also detected whose peak activity was detected in cortices prepared from zygotes undergoing cytokinesis. In addition, $p34^{cdc2}$ was detected in cortices by Western blotting. To further examine the kinetics of cortical H1 kinase activity, zygotes of the sand dollar *E. parma* were harvested at various times after fertilization, and whole cell and detergent-extracted cytoskeletons were prepared for analysis. As shown in Fig. 1 A, a consistent delay in peak activity was observed in the cytoskeletal fractions when compared with whole cell H1 kinase activities through the first two cell cy-

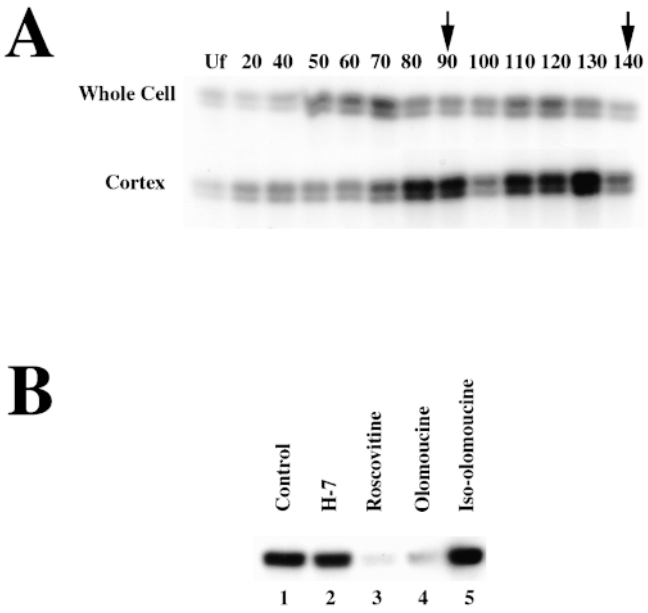

Figure 1. Characterization of cortical histone H1 kinase activity. (A) At the times either before (Uf) or following fertilization (20–140 min after fertilization), zygotes were washed and both whole cell lysates and detergent-extracted cytoskeletons were prepared, snap frozen, then assayed for H1 kinase activity. The first and second cleavages occurred at 90 and 140 min after fertilization, and are denoted with arrows. (B) Detergent-extracted cortical cytoskeletons prepared from dividing blastomeres were assayed for H1 kinase activity in the presence of 10 μM H-7, 5 μM roscovitine, 10 μM olomoucine, or 10 μM isoolomoucine. Note that while the PKC inhibitor H-7 has no effect on H1 kinase activities, the CDK inhibitors roscovitine and olomoucine (but not the inactive isomer, isoolomoucine) strongly inhibit H1 kinase activity.

cles. Although the actual times at which cleavage occurred varied slightly from one experiment to another due to differences in the temperature at which the zygotes were cultured, cortical H1 kinase activity peaked on average 10–15 min after whole cell levels had reached maximum levels. Observation of embryos collected at this time by interference contrast microscopy indicated that cells had entered anaphase and many had begun dividing. These differential kinetics between whole cell and cytoskeletal-associated H1 kinase activity was not species-specific, but were also observed in all species of sea urchins tested (*Strongylocentrotus purpuratus, L. pictus, Lytechinus variegatus*).

To confirm that this activity was attributable to $p34^{cdc2}$ and not other kinases present in the cortex, we tested the cortical H1 kinase activity in the presence of a battery of kinase inhibitors, including several derivatives of 6-dimethylamino purine (6-DMAP), whose effects are specific to cyclin-dependent kinases, including $p34^{cdc2}$ (Meijer et al., 1997). As shown in Fig. 1 B, cortical H1 kinase activity was sensitive to the CDK inhibitors roscovitine, olomoucine, and butyrolactone (data not shown), but not the inactive isomer isoolomoucine or the PKC/PKA inhibitor H-7. Cortical H1 kinase activity is also insensitive to the MLCK inhibitor ML-9, and genistein (data not shown). In addition, measurements of specific activities indicate that cortical H1 kinase activity was enriched on average 2.5–3-fold over whole cell levels.

Myosin Light Chain Phosphorylation during Mitosis

Results of H1 kinase assays indicated that cytoskeletal-associated $p34^{cdc2}$ activity cycled with kinetics delayed with respect to whole cell levels, and that this delayed activity extended into anaphase and cleavage. In light of data suggesting that $p34^{cdc2}$ may regulate the timing of cytokinesis through the modulation of myosin II activity (Satterwhite et al., 1992; Yamakita et al., 1994), we asked whether the extended $p34^{cdc2}$ activity is reflected in vivo by myosin regulatory light chain (LC20) phosphorylation in the cortical cytoskeleton of sea urchin embryos. Smooth muscle and cytoplasmic myosin light chains may be phosphorylated on five residues: serines 1 and 2, threonine 9, threonine 18, and serine 19 (for reviews see Sellers, 1991; Satterwhite and Pollard, 1992; Bresnick, 1999). Whereas PKC phosphorylates LC20 on serines 1 and 2 and threonine 9 (Nishikawa et al., 1984; Bengur et al., 1987; Ikebe and Reardon, 1990), $p34^{cdc2}$ phosphorylates serines 1 and 2 only (Satter-

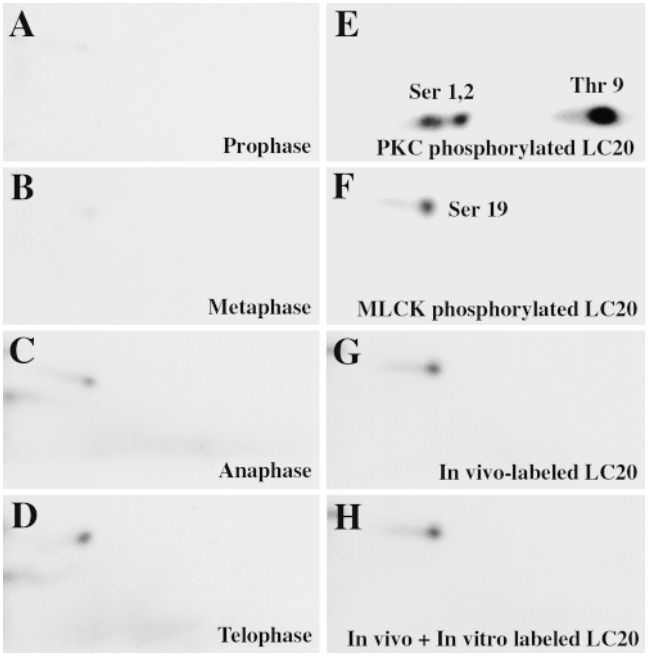

Figure 2. In vivo analysis of cortical myosin light chain phosphorylation. (A–D) *L. pictus* eggs were incubated in the presence of $^{32}PO_4$ in phosphate-free artificial sea water. Cells were monitored with interference contrast optics, and at time points when the cells were in (A) prophase, (B) metaphase, (C) anaphase, and (D) telophase (69, 78, 85, and 95 min after fertilization, respectively). Zygotes were washed and cortical cytoskeletons prepared from each time point. Cortical protein was resolved by SDS-PAGE, and light chains were excised, and digested with TPCK-trypsin. Digests were then washed and subjected to two-dimensional peptide analysis on cellulose TLC plates. The designations of the phosphopeptides are based on Satterwhite (1992). (E and F) Purified myosin II was phosphorylated in vitro using purified PKC (E) or MLCK (F). Peptide digests of cortical LC20 labeled in vivo were analyzed either alone (G) or mixed with equal counts of LC20 phosphorylated in vitro with MLCK (H).

white et al., 1992). In contrast, MLCK phosphorylates both threonine 18 and serine 19 (Sellers, 1991). These differential phosphorylation sites may be resolved by phosphopeptide mapping as illustrated in Fig. 2, where purified myosin II was phosphorylated in vitro by PKC or MLCK. Two phosphopeptides were detected in PKC phosphorylated light chains, corresponding to serines 1 and 2 and threonine 9 (Fig. 2 E), whereas a single phosphopeptide corresponding to serine 19 was visible in light chains phosphorylated by MLCK (Fig. 2 F) (Satterwhite et al., 1992). Peptide digests from in vitro–phosphorylated brush border or sea urchin egg myosin II were superimposable when phosphorylated by the same kinases (data not shown), indicating that the sea urchin homologue of regulatory light chain also contained these positive and negative regulatory sites.

Using metabolic labeling and phosphopeptide mapping, we followed the phosphorylation of regulatory light chain in the cortical cytoskeleton of sea urchin zygotes through mitosis. Synchronous, metabolically labeled cultures were monitored by interference contrast optics, and samples were collected at the time of nuclear envelope breakdown, metaphase, anaphase, and cleavage. Cortical cytoskeletons were prepared from each sample, and after SDS-PAGE and transfer to polyvinylidene difluoride (PVDF) membranes, light chains were subjected to tryptic digestion and peptide mapping. As shown in Fig. 2, there was little detectable light chain phosphorylation up until anaphase, at which time there was a dramatic increase in a single phosphopeptide (Fig. 2 C). Mixing tryptic digests from MLCK-phosphorylated light chains (Fig. 2 F) with in vivo–labeled LC20 digests prepared from telophase zygotes (Fig. 2 G) identified the phosphopeptide in anaphase and telophase as the activating MLCK site (Fig. 2 H). Serine 19 phosphorylation decreased after cleavage (110–125 min after fertilization), and the fluctuations in cortical LC20 phosphorylation could not be attributed to differences in myosin II recruitment to the cortex, since Western blotting of in vivo–labeled cortices revealed that levels of myosin II remained constant throughout the cell cycle (data not shown).

Although the increase in LC20 phosphorylation on activating residues is consistent with data from cultured cells where there is an increase in serine 19 phosphorylation upon anaphase onset (DeBiasio et al., 1996; Matsumura et al., 1998; Murata-Hori et al., 1998), we were surprised to find no evidence of serine 1,2 phosphorylation on light chains associated with cytoskeletal myosin heavy chain at any time during mitosis (Fig. 2), especially in light of our data regarding $p34^{cdc2}$ activity associated with cytoskeleton (Fig. 1 A). Light chain phosphorylation on serine 1,2 has been detected in vivo in tissue culture cells arrested in mitosis using microtubule-destabilizing drugs (Yamakita, 1994), as well as *Xenopus* (Satterwhite, 1992) and sea urchin (Mishima and Mabuchi, 1996; Totsukawa et al., 1996) extracts. This apparent discrepency might be explained by either: (a) the soluble and cytoskeletal myosin populations were subject to differential regulation; (b) the presence of a phosphatase activity that prevented our detection of cdc2 phosphorylation of light chain; or (c) a selective destabilization or solubilization of myosin filaments from the cortical cytoskeleton following serine 1,2 phosphorylation

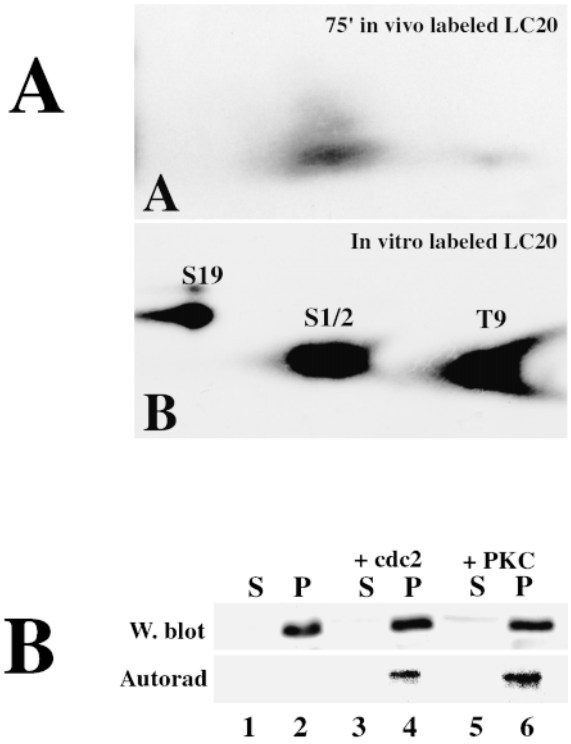

Figure 3. Compartmentalization of serine 1,2 phosphorylation. (A) *L. pictus* eggs were incubated in the presence of inorganic $^{32}PO_4$ in phosphate-free artificial sea water. Zygotes were cultured up to metaphase of the first cell division, washed, and lysed in a buffer containing 0.5% NP-40 and protease and phosphatase inhibitors. Cortical cytoskeletons were removed by centrifugation, and myosin II was isolated from the supernatant by immunoprecipitation. Light chains were subjected to proteolysis and two dimensional phosphopeptide analysis. (A, panel A) LC20 immunoprecipitated from metaphase zygotes (77 min after fertilization). (A, panel B) LC20 phosphorylated in vitro with both PKC and MLCK to identify both activating and inhibitory phosphorylation sites. (B) Cortices were prepared from interphase zygotes (30 min after fertilization) and incubated with [γ-^{32}P]ATP in the absence (lanes 1 and 2) or presence of purified $p34^{cdc2}$ (lanes 3 and 4) or PKC (lanes 5 and 6) for 30 min. The suspension was then clarified by centrifugation, and the supernatant (lanes 1, 3, and 5) and pellet (cytoskeletal) fractions (lanes 2, 4, and 6) were analyzed by Western blotting and autoradiography.

(Nishikawa et al., 1984; Bengur et al., 1987; Ikebe and Reardon, 1990). To control for the first two possibilities, sea urchin eggs were labeled in vivo, samples collected from cultures during metaphase, and LC20 was immunoprecipitated from detergent-soluble supernatants using anti–myosin heavy chain antibodies and subjected to tryptic digestion and phosphopeptide analysis. As shown in Fig. 3 A, a major phosphopeptide could be detected in samples prepared from metaphase zygotes (Fig. 3 A, panel A) that comigrated with phosphopeptides derived from in vitro–phosphorylated LC20 (Fig. 3 A, panel B). A second, minor phosphopeptide could be detected comigrating with threonine 9–containing phosphopeptides. These results suggested that our experimental conditions did allow for the detection of serine 1,2 phosphorylation in vivo, and suggested that serine 1,2 modulation of myosin II activity

may be dependent on the cytoplasmic compartment in which the myosin molecules reside.

Finally, experiments were performed in vitro to control for the possibility that $p34^{cdc2}$ phosphorylation of LC20 might selectively destabilize myosin II association with the cortical cytoskeleton, and thus preclude our detection of serine 1,2 phosphorylation in the cortex. Cortices were prepared from zygotes at times when cortical kinase activity is low in comparison to dividing cells (20–50 min after fertilization) (Walker et al., 1997), and treated with purified $p34^{cdc2}$–cyclin B or PKC in the presence of [γ-^{32}P]ATP. The reactions were then clarified by low speed centrifugation, and the supernatant and pellet (cortical) fractions examined by autoradiography and Western blotting with an anti–egg myosin antibody that recognizes both heavy and light chains. As shown in Fig. 3 B, there was no detectable increase in soluble myosin as the result of either $p34^{cdc2}$ or PKC treatment. Autoradiography confirms that LC20 phosphorylation was detectable in both $p34^{cdc2}$- and PKC-treated cortices, confirming that the cytoskeletal-associated myosin light chains were accessible to the soluble kinases. Thus, LC20 phosphorylation on inhibitory sites did not appear to correlate with an increase in myosin solubility.

Induction of Cleavage Furrows in Mitotically Arrested Cells

Results of in vivo labeling and phosphopeptide mapping suggest that despite the enriched and extended levels of $p34^{cdc2}$ activity associated with the cortex, cytoskeletal myosin II was not subject to a light chain-based negative regulation during mitosis. In an effort to directly assess the light chain–based model for the timing of cytokinesis in vivo, we asked whether the cortex could be induced to form a cleavage furrow in the presence of chronically extended $p34^{cdc2}$ activity. Towards these ends, a truncated, nondegradable form of cyclin B was produced in *Escherichia coli* (Δ90 cyclin) (Murray et al., 1989; Glotzer et al., 1991). Nondegradable forms of cyclin B have been introduced in cultured cells as well as *Xenopus* and sea urchin eggs (Murray et al., 1989; Wheatley et al., 1997; Hinchcliffe, 1998). In each case, chromatin remains condensed, and cleavage is arrested. However, because there are dramatic effects on microtubule dynamics and spindle behavior in Δ90 cyclin–arrested cells, it is difficult to attribute the inhibition of cytokinesis to either a suppression of myosin II–based contractility or a failure to deliver the cleavage stimulus to the cortex. To differentiate between these possibilities, recombinant Δ90 cyclin was produced in bacteria, purified to homogeneity, and tested in *Xenopus* cell–free extracts for its ability to arrest cycling extracts in a mitotic state (data not shown). Δ90 cyclin was then concentrated and injected into blastomeres of two cell *E. parma* embryos. Injection of Δ90 into blastomeres shortly before nuclear envelope breakdown resulted in mitotic arrest in 81% of the cells injected (n = 42). In six cases where Δ90 cyclin was injected during metaphase, cells divided but arrested in the following cell cycle. In contrast, 93% of cells injected with buffer alone (n = 31) went on to develop past the mesenchymal blastula stage. Examination of injected cells revealed that although injected blastomeres failed to divide, the mitotic apparatus was still visible and spindle poles underwent an anaphase B–like separation as reported previously (Holloway et al., 1993; Wheatley et al., 1997; Hinchcliffe, 1998), and in some cases, the spindle poles split to form three or four individual aster centers (Fig. 4 A). Arrested blastomeres remained viable for up to 3 h, at which time the cells underwent membrane blebbing, and died soon after (Hinchcliffe et al., 1998). Vital staining with Hoescht No. 33342 revealed that throughout this period, chromatin remained condensed.

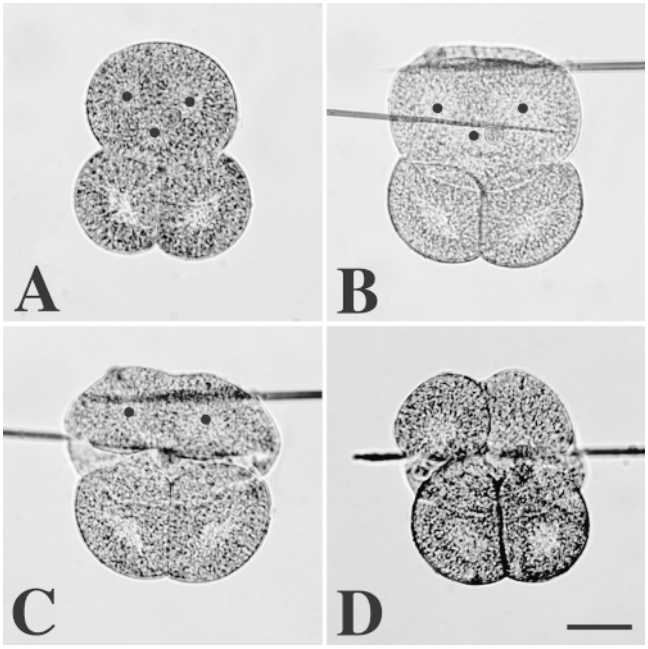

Figure 4. Mitotic arrest and needle displacement in Δ90 cyclin-injected sand dollar embryos. Zygotes were cultured at 15°C through the first division. Shortly before prophase of the second cell division, one blastomere was injected with Δ90 cyclin B and marked by a small oil droplet. 35 min after the second division of the control blastomere (at 150 min after fertilization), small asters remain visible in the Δ90-injected embryo, and a third aster is visible, most likely the result of spindle pole splitting (Hinchcliffe, 1998) (A). Needles were then placed across the surface, isolating two aster centers and forcing them into a confined region of cytoplasm (B). 5 min after the initial displacement, a unilateral furrow becomes visible, which continues to ingress after one needle is removed (C and D). The control blastomeres went on to divide 10 min later. Dots indicate the position of the aster centers in the injected blastomere. Bar, 30 μm.

To ask whether cells arrested in mitosis were capable of forming cleavage furrows, Δ90-injected blastomeres were manipulated such that the spindle poles were placed in close proximity to the cell surface. To perform this manipulation, two opposing needles were brought down upon the surface of the injected blastomere, and pressed down so that two aster centers were isolated within a confined space and pushed against the surface. As shown in Fig. 4, a unilateral furrow formed between the spindle poles. If one or both needles are removed once furrowing commences, the furrow progressed to near completion. Arrested blas-

tomeres induced to furrow in this fashion remain arrested, and underwent no further divisions. Furrowing occurred ~5 min after application of the needles, resembling the normal kinetics of cleavage furrow induction in *E. parma* embryos (Rappaport and Ebstein, 1965; Rappaport and Rappaport, 1993). Of the 14 Δ90-arrested blastomeres manipulated in this fashion, 8 were induced to furrow. Of the blastomeres that failed, two had asters that were normal to plane of the pipettes (and the coverslip) such that the furrow would have to ingress along the long axis of the bisected cell. The remaining four cells had spindle poles that had separated >45 μm, a distance determined previously in normal *E. parma* blastomeres to be too great to induce furrowing (Rappaport, 1969).

The physical manipulation of the asters in Δ90-arrested cells suggested not only that the cortical cytoskeleton retains the capacity to assemble a contractile ring in the presence of chronically elevated MPF levels, but also suggested that the timing of cytokinesis may be a function of the spindle's capacity to deliver the signal to the surface. To further explore this notion, a second method was employed to alter the geometry of normal and Δ90-arrested cells. Blastomeres were carefully drawn into a fire-polished capillary pipette, resulting in a cylindrical cell and a reduced distance between the spindle pole and the cell surface (Rappaport, 1981, 1997). As shown in Fig. 5, when an uninjected blastomere was drawn into a pipette, the mitotic apparatus is usually drawn into the distal portion of the cell. Just after the appearance of anaphase asters (Fig. 5 B), a cleavage furrow was induced and furrowing was complete before the spherical control had commenced cleavage, even though anaphase onset and astral microtubule elongation occurred simultaneously in the two cells. When Δ90-arrested cells were drawn into a pipette, cleavage furrows could also be observed. In the embryo shown in Fig. 6, the aster centers could not be clearly delineated, but a localized contraction was induced adjacent to a cleared zone (arrow), and because the spindle was aligned slightly oblique to the axis of the cylinder, the furrow attempted to progress along the long axis of the cell. Similar results have been obtained with normal cylindrical cells when the axis of the spindle is normal to the long axis of the cell (Rappaport and Ratner, 1967; Rappaport and Rappaport, 1987). Similar results were obtained using injected mRNA in *L. pictus* and *Dendraster excentricus.* Furrows induced in cylindrical, Δ90-injected embryos were irregular, and while none (5/5 blastomeres) progressed to completion, contractility activity was observed in all cells whose capillary diameter was not >60 μm.

Discussion

In an effort to understand the role of protein phosphorylation in the temporal and spatial regulation of cleavage furrow formation, we sought to address how $p34^{cdc2}$ kinase affects the timing of contractile ring assembly in embryonic cells. Results of this study indicate that despite enriched and prolonged levels of $p34^{cdc2}$ activity associated with the cortical actin cytoskeleton, there is no appreciable phosphorylation of myosin regulatory light chain on residues shown to be inhibitory for myosin II motor activity (Bengur et al., 1987; Nishikawa et al., 1987). Additionally, micromanipulation and microinjection studies with nondegradable forms of cyclin B indicate that cells arrested in mitosis are capable of forming cleavage furrows, but do not do so unless mitotic apparatus is in direct contact with the cell surface. Together, these results represent a critical assessment of the respective roles of $p34^{cdc2}$ and myosin II regulation in the timing of cytokinesis, and suggest that while the programmed destruction of $p34^{cdc2}$ activity may indeed act as the timer for cytokinesis, the timing of cytokinesis is not accomplished by a suppression of myosin II–based contractility.

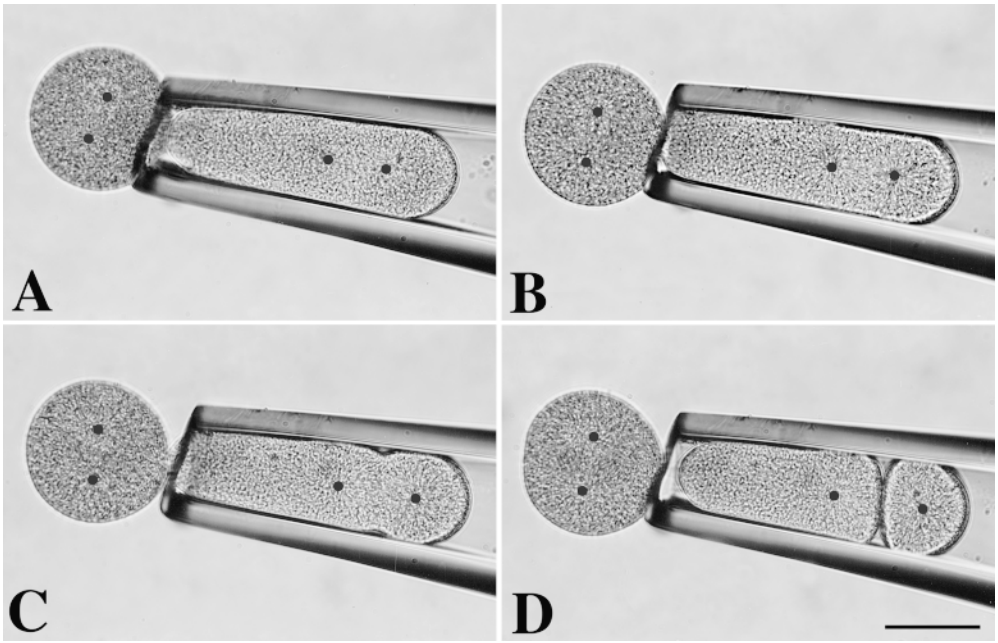

Figure 5. Cleavage formation in a cylindrical cell. Zygotes were cultured through the first division at 15°C. Upon appearance of a mitotic spindle, one blastomere was drawn into a fire-polished capillary pipette. At 150 min after fertilization, the anaphase asters become visible, and a bilateral furrow appears shortly afterward. Note that by the time the control blastomere begins to cleave (D), the cylindrical blastomere has completed cytokinesis. (A–D) 145, 150, 153, and 159 min after fertilization, respectively. Dots indicate the positions of the aster centers. Bar, 80 μm.

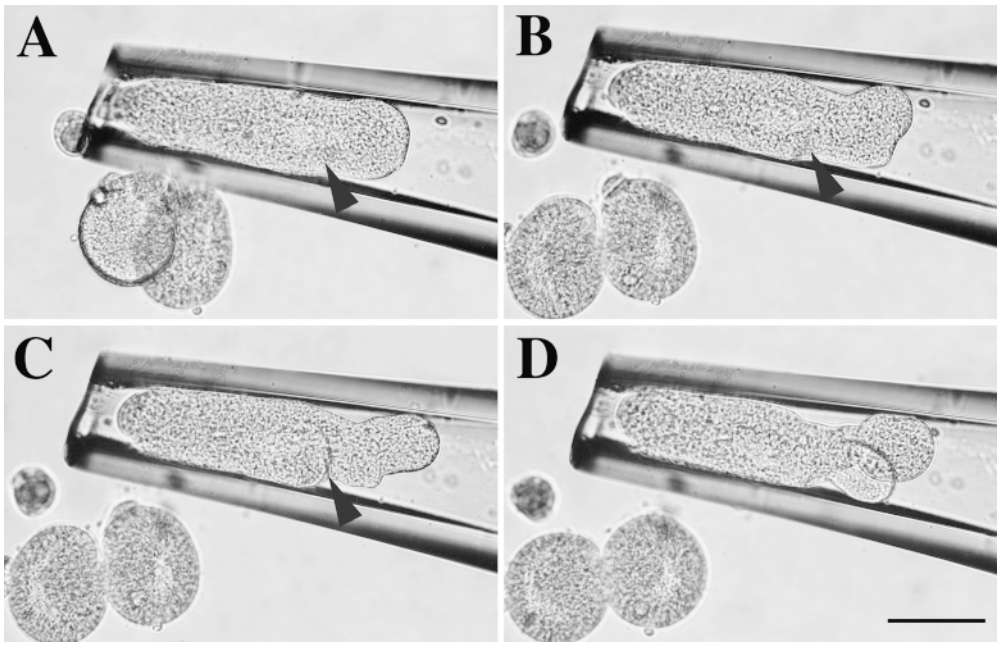

Figure 6. Cleavage furrow formation in a cylindrical, Δ90-arrested cell. One blastomere of a two cell embryo was injected with Δ90 cyclin, and 30 min after cleavage of the uninjected control, the arrested cell was drawn into a pipette. Although the exact position of the aster centers is not clearly visible in this specimen, the arrows indicate a cleared zone in the cytoplasm, where ~3 min later, a furrow becomes visible that progresses along the long axis of the cell. (A–D) 190, 193, 197, 201 min after fertilization, respectively. Bar, 80 μm.

Spatial Differences in p34^{cdc2} Activation and the Regulation of the Cortical Cytoskeleton

Mapping of cortical and whole cell H1 kinase activity indicates that p34^{cdc2} activity associated with the actin cytoskeleton cycles with kinetics delayed with respect to global MPF levels (Fig. 1). Whether this activity is sequestered within a specific subdomain of the cortex (i.e., polar versus equatorial), or what the functional significance of this delayed activity is in regards to the spatio-temporal regulation of contractile ring formation remains unknown at this time. The notion that cyclin destruction does not proceed uniformly throughout the cytoplasm has been recently demonstrated in *Drosophila* embryos where cyclin destruction begins at the spindle poles and spreads to the spindle midzone, after which cyclin disappears from the cytoplasm (Huang and Raff, 1999). Actin-associated MPF activity may represent a sequestered fraction of activity that is last to undergo ubiquitin-mediated destruction.

In amphibian eggs, MPF activation is not only spatially regulated, but is also associated with a reorganization of the cortical cytoskeleton. A series of surface contraction waves (SCWs) originate from the animal pole in a cell cycle–dependent manner during the early cleavage cycles of frog and salamander embryos (Hara, 1971; Hara et al., 1980). Subsequent mapping of surface contractile behavior and p34^{cdc2} activity indicates that the wave of MPF activation originating at the animal pole runs concomitantly with a relaxation of the cortex (SCWa) (Rankin and Kirschner, 1997; Pérez-Mongiovi et al., 1998). Conversely, cyclin B destruction is accompanied by a cytochalasin-insensitive contraction wave (SCWb) (Christensen and Merriam, 1982; Rankin and Kirschner, 1997; Pérez-Mongiovi et al., 1998). While these waves run concomitantly with the division cycle, the biochemical nature of these cycles of cortical relaxation and contraction, as well as their relatedness to contractile ring formation, is still unclear (Christensen and Merriam, 1982; Asada-Kubota and Kubota, 1991). It is yet to be determined whether myosin light chain phosphorylation also accompanies either the relaxation or contraction waves. Additionally, the actin-binding proteins caldesmon and spectrin have both been shown to be substrates of p34^{cdc2}, and this modulation negatively regulates the interactions of these proteins with the actin cytoskeleton (Yamashiro et al., 1991; Fowler and Adam, 1992). It is conceivable then that the cortical relaxation observed with MPF activation is attributable to the modulation of filament binding and cross-linking proteins. With regard to echinoderm eggs, the inverse trend towards increased cortical stiffness during mitosis (Hiramoto, 1990) does not seem to correlate either to myosin light chain phosphorylation in the cortex (Fig. 2), or to the ability of the cortex to respond to signals from the mitotic apparatus (Rappaport, 1985). Further characterization of cortical H1 kinase activity in echinoderm eggs, as well as identification of other cortical substrates for p34^{cdc2}, will reveal whether the differential activation and inactivation of cortical p34^{cdc2} is related to the spatial regulation of MPF activity seen in *Xenopus* eggs.

Myosin II Regulation during Mitosis

In vivo analysis of myosin light chain phosphorylation reveals that whereas there was evidence of p34^{cdc2} phosphorylation on light chains associated with soluble myosin II, cortical-associated myosin was under no such regulation despite the presence of p34^{cdc2} activity associated with the actin cytoskeleton (Fig. 2 and Fig. 3 A). Control experiments suggest that the absence of serine 1,2 phosphorylation in cortical LC20 is not due to altered solubilities of phosphorylated myosin, accessibility of serines 1 and 2 to phosphorylation, or artifacts of preparation that would

preclude our detection of serine 1,2 phosphorylation (Fig. 3). In vitro, regulatory light chain is a poor substrate for $p34^{cdc2}$ when associated with myosin heavy chain (Yamakita et al., 1994), yet robust serine 1,2 phosphorylation can be detected in sea urchin (Mishima and Mabuchi, 1996; Totsukawa et al., 1996) and *Xenopus* (Satterwhite et al., 1992) extracts, as well as in whole cell extracts from metabolically labeled tissue culture cells (Yamakita et al., 1994). However, the induction of cleavage furrows in Δ90-injected cells argues that the model proposing $p34^{cdc2}$-mediated suppression of myosin II activity and thus cytokinesis may no longer represent a viable one for the timing of cytokinesis, regardless of the cytoplasmic compartment in which the regulation occurs. Indeed, a recent study carried out in fission yeast indicates that mutations in the light chain phosphorylation sites have no effects on cytokinesis (McCollum et al., 1999). It is possible that differential regulation of cytoskeletal and soluble myosin II may contribute to the tight spatial regulation of myosin activation and contractile ring formation in embryonic cells. Embryos generally contain large stores of contractile proteins required for the rapid series of cell divisions that accompany early development, and ~90% of myosin II is soluble in the sea urchin egg (Shuster, C., unpublished observations). Inactivation of this large soluble pool may contribute to spatial regulation of cleavage furrow formation by limiting the myosin filaments that may be activated or recruited to the cleavage furrow. If this is indeed the case, serine 1,2 phosphorylation would likely accomplish this by lowering the affinity of myosin for actin, and not by affecting the ability of MLCK to phosphorylate light chain (Turbedsky et al., 1997).

Another issue regarding the regulation of myosin II during cell division centers on the role of serine 19 phosphorylation during cytokinesis. Studies using phosphoepitope-specific antibodies for serine 19 as well as phosphorylation-sensitive biosensors detect an increase in serine 19 phosphorylation upon anaphase onset that concentrates in the equatorial zone as well as in the margins as the cells respread following mitosis (DeBiasio, 1996; Matsumura et al., 1998). The kinetics of serine 19 phosphorylation in the cortical cytoskeleton of sea urchin embryos resemble those seen in cultured cells (Fig. 2). And although there is a correlative relationship between serine 19 phosphorylation and cytokinesis, studies of regulatory light chain function in *Dictyostelium* argue that light chain phosphorylation may be altogether dispensable for contractile ring function (Uyeda and Spudich, 1993; Ostrow et al., 1994). While basal levels of actin-activated ATPase activity may be sufficient for contractile ring formation in *Dictyostelium* grown either on substrate or in suspension (Ostrow et al., 1994), the role of serine 19 phosphorylation in mammalian cells as well as in echinoderm eggs has not been thoroughly evaluated. Mutation of both MLCK sites in *Drosophila* results in defects in cytokinesis and ring canal formation resembling the light chain–null (*spaghetti-squash)* phenotype (Karess et al., 1991; Jordon and Karess, 1997), suggesting that activating phosphorylation is required for cytokinesis. Testing the functional significance of serine 19 phosphorylation during cell division in animal cells, and the unequivocal identification of the modifying kinase are both areas of intense interest and investigation (Bresnick, 1999).

Delivery of the Cleavage Stimulus and the Timing of Cytokinesis

The induction of cleavage furrows in Δ90-arrested cells supports the notion that the cortex is capable of responding to contractile stimuli even under conditions of chronically elevated MPF levels, and corroborate biochemical data indicating that cortical myosin II is not under a light chain–based suppression during mitosis (Fig. 2). Introduction of nondegradable cyclin B (Δ90 cyclin) into dividing echinoderm eggs or tissue culture cells results in a stereotypic series of spindle movements where sister chromatid separation proceeds normally as does anaphase B spindle movements, but the nuclear envelope does not reform and cytokinesis does not occur (Wheatley et al., 1997; Hinchcliffe et al., 1998; this report). Spindle pole separation becomes quite exaggerated, and in the case of echinoderm embryos, spindle poles split to form up to four asters (Hinchcliffe et al., 1998) (Fig. 4). As a means of assessing whether the cortical cytoskeleton can respond to signals from the spindle in the presence of high MPF levels, the geometrical relationship between the spindle and the cell surface was altered in Δ90-arrested blastomeres (Figs. 4 and 6). Under conditions where aster centers were placed adjacent to the cortex, furrows could be induced at the equatorial zone between the spindle poles (Fig. 4). The induction of cleavage furrows was not only dependent upon reducing the distance between the spindle pole and the surface, but also on the interastral distance, where furrowing could not be induced in cells where extreme anaphase B spindle pole separation could not be compensated for by pushing the asters against surface (data not shown). In this sense, our data support the argument made by Wheatley et al. (1997) that the cytokinesis defect in Δ90-injected cells is due to exaggerated anaphase B movements that reduce the capacity of the microtubules (astral microtubules in sea urchin eggs, midzone microtubules in tissue culture cells) to stimulate cleavage furrows. However, we observed many cases (n = 15) where spindle poles split to form multiple asters (see Fig. 4 A), all of which had interastral distances which would normally support furrow formation (29–35 μm), but the cells did not divide unless the asters were physically displaced toward the cortex. Thus, it appears that spindle integrity alone does not explain the reversible inhibition of cleavage furrows in Δ90-arrested blastomeres.

The necessity of bringing the asters of Δ90-injected cells into close proximity with the cortex suggests that at least one determinant of the timing of cytokinesis is the geometrical relationship between the spindle poles and the surface. The spatial relationship between the spindle poles and the surface in normal and geometrically or chemically altered cells, and the respective effects on the timing of cleavage furrow formation is illustrated in Fig. 7. Under normal conditions, the cleavage plane is specified shortly after the metaphase–anaphase transition (Rappaport, 1996). With the onset of anaphase and the decline of $p34^{cdc2}$ activity, there is an extensive elaboration and elongation of astral microtubules along with an accompanying

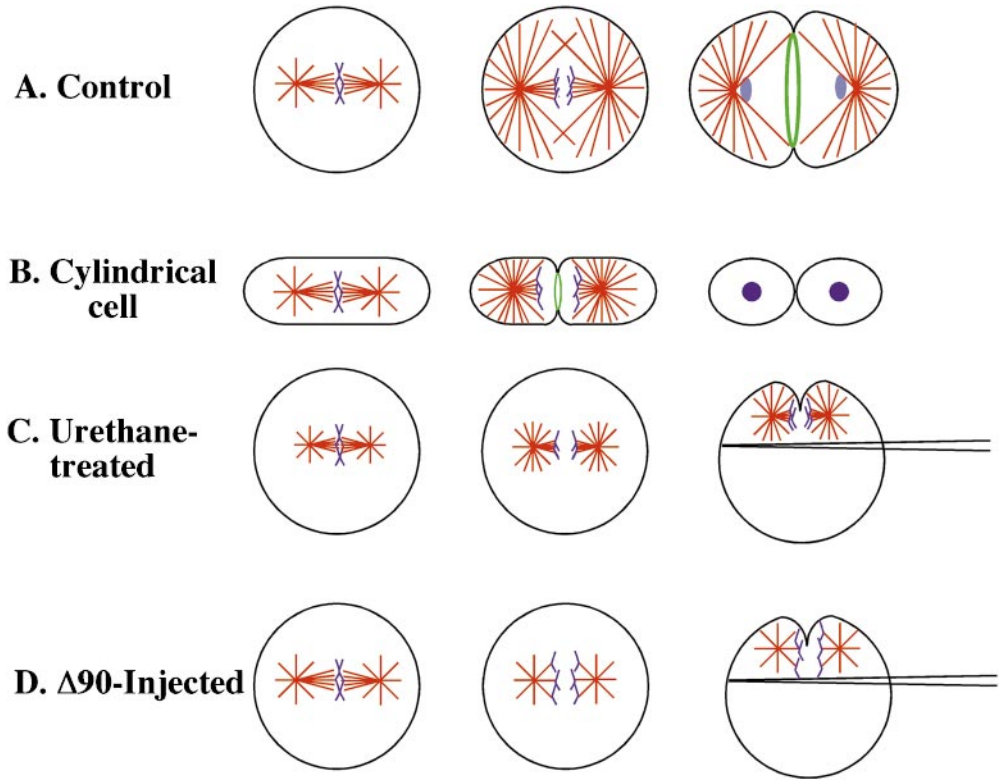

Figure 7. Spatial relationships between the spindle poles and the cell surface specify the timing of cytokinesis in echinoderm eggs. (A) In spherical control blastomeres, the onset of anaphase is accompanied by an elaboration of astral microtubules that contact the surface. After a short latent period, a cleavage furrow forms that ingresses to completion in ~7 min. (B) If blastomeres are manipulated into a cylindrical form, the distance between the spindle poles and the surface is reduced, and a furrow forms precociously in comparison with spherical controls (this report). (C) Treatment of mitotic sand dollar eggs with 60 mM urethane results in an inhibition of astral microtubule elongation (Rappaport, 1971; Rappaport and Rappaport, 1984) and a failure to cleave. The inhibition of cytokinesis may be overcome by physically shifting the position of the mitotic apparatus towards the surface. (D) Blastomeres arrested in mitosis by injection of Δ90 cyclin B undergo normal chromosome separation and anaphase B movements, but the spindle fails to induce a furrow (Wheatley et al., 1997; Hinchcliffe et al., 1998; this report). However, reduction of the distance between the spindle poles and the surface may overcome the inhibition of cleavage by physical displacement of the asters towards the surface.

loss of spindle birefringence (Fig. 7 A) (Salmon and Wolniak, 1990). Contact between astral microtubules and the surface requires as little as 1 min to specify the position of the furrow, and after a brief latent period the contractile ring is induced (Rappaport and Ebstein, 1965). Under conditions where the distance between the spindle poles and the surface is reduced, as in the case of a cylindrical cell (Fig. 7 B), contractile rings are induced and progress to completion before spherical controls (Fig. 5). Thus, while both spherical and cylindrical cells enter anaphase at the same time, the timing of furrow formation is a function of the distance that the putative cleavage stimulus has to travel to reach the surface, and not an abrupt cell cycle transition.

Chemical modulations of astral microtubule elongation extend this notion. If astral microtubule elongation is inhibited with reagents such as urethane (Rappaport, 1971; Rappaport and Rappaport, 1984), cytokinesis does not occur unless the distance between the spindle pole and the surface is reduced by micromanipulation (Fig. 7 C). One explanation for the reversible inhibition of cytokinesis observed in Δ90-arrested blastomeres is that the physical displacement of the spindle poles towards the surface compensates for the normal elaboration of the astral microtubules during anaphase (Fig. 7 D). Collectively, the induction of cleavage furrows under these conditions implicates the delivery of the cleavage stimulus via astral microtubule elongation as an important determining factor in the timing of cytokinesis. Therefore, by implication, the regulation of microtubule dynamics represents an indirect mechanism by which the timing of cytokinesis may be specified by $p34^{cdc2}$.

The rates of microtubule turnover shift dramatically during mitosis (for reviews see Desai and Mitchison, 1997; Cassimeris, 1999), and the 10-fold increase in microtubule catastrophe rates seen in cell-free extracts is dependent on $p34^{cdc2}$ (Belmont et al., 1990; Belmont and Mitchison, 1996; Verde et al., 1990). Indeed, $p34^{cdc2}$–cyclin B has been shown to bind and phosphorylate both microtubule-associated protein 4 (Vandré et al., 1991; Ookata et al., 1995) and p77 echinoderm microtubule-associated protein (Brisch et al., 1996), and MAP kinase family members have also been implicated in the regulation of microtubule dynamic instability (Gotoh et al., 1991; Brisch et al., 1999). Phosphorylation lowers the affinity of MAPs for the microtubule, resulting in increasing catastrophe rates (McNally, 1996). However, additional factors such as Op18 (Belmont and Mitchison, 1996), the kinesin-like protein XKCM1 (Walczak et al., 1996), and the microtubule-severing protein katanin (McNally and Vale, 1993; McNally and Thomas, 1998) may also play crucial roles in regulating microtubule stability during mitosis. The notion that microtubule turnover remains at a mitotic state in Δ90-arrested cells is supported by observations of injected sea urchin zygotes with polarization optics (Hinchcliffe et al., 1998), where the spindle undergoes normal anaphase chromosome separation,

yet the spindle poles remain birefringent. Understanding how the activities of these factors change in relation to the fall of MPF activity during anaphase may identify critical regulatory events that lead to the stabilization of astral microtubule arrays and induction of contractile ring assembly.

The authors would like to thank Drs. Mike Glotzer and Karl Fath for their generosity in sharing reagents. A great debt of gratitude is owed to Ray Rappaport for sharing his thoughts, time, and equipment at the Mount Desert Island Biological Laboratory.

This work was supported by a National Institutes of Health National Research Service Award (GM18823) to C.B. Shuster and a Mount Desert Island Biological Laboratory New Investigator's award and National Institutes of Health grant GM58231 to D.R. Burgess.

Submitted: 4 June 1999
Revised: 3 August 1999
Accepted: 5 August 1999

References

Asada-Kubota, M., and H.Y. Kubota. 1991. Furrow-related contractions are inhibited but furrow-unrelated contractions are not affected in *af* mutant eggs of *Xenopus laevis. Dev. Biol*. 147:354–362.

Belmont, L.D., and T.J. Mitchison. 1996. Identification of a protein that interacts with tubulin dimers and increases the catastrophe rates of microtubules. *Cell*. 84:623–631.

Belmont, L.D., A.A. Hyman, K.E. Sawin, and T.J. Mitchison. 1990. Real time visualization of cell cycle-dependent changes in microtubule dynamics in cytoplasmic extracts. *Cell*. 62:579–589.

Bengur, A.R., E.E. Robinson, E. Appella, and J.R. Sellers. 1987. Sequence of the sites phosphorylated by protein kinase C in the smooth muscle light chain. *J. Biol. Chem*. 262:7613–7617.

Bresnick, A.R. 1999. Molecular mechanisms of nonmuscle myosin-II regulation. *Curr. Opin. Cell Biol.* 11:26–33.

Brisch, E., M.A.F. Daggett, and K.A. Suprenant. 1996. Cell cycle-dependent phosphorylation of the 77 kDa echinoderm microtubule-associated protein (EMAP) in vivo and association with cdc2 kinase. *J. Cell Sci*. 109:2885–2893.

Brisch, E., D.P. Ahrens, and K.A. Suprenant. 1999. Phosphatase-sensitive regulators of microtubule assembly copurigy with sea urchin egg microtubules. *J. Exp. Zool.* 283:258–269.

Cao, L.-G., and Y.-L. Wang. 1996. Signals from the spindle midzone are required for the stimulation of cytokinesis in cultured epithelial cells. *Mol. Biol. Cell*. 7:225–232.

Cassimeris, L. 1999. Accessory protein regulation of microtubule dynamics throughout the cell cycle. *Curr. Opin. Cell Biol.* 11:134–141.

Christensen, K., and R.W. Merriam. 1982. Insensitivity to cytochalasin B of surface contractions keyed to cleavage in the *Xenopus* egg. *J. Embryol. Exp. Morphol.* 72:143–151.

DeBiasio, R.L., G.M. LaRocca, P.L. Post, and D.L. Taylor. 1996. Myosin II transport, organization, and phosphorylation: evidence for cortical flow/solation-contraction coupling during cytokinesis and cell locomotion. *Mol. Biol. Cell*. 7:1259–1282.

Desai, A., and T.J. Mitchison. 1997. Microtubule polymerization dynamics. *Annu. Rev. Cell Biol.* 13:83–117.

Field, C., R. Li, and K. Oegema. 1999. Cytokinesis in eukaryotes: a mechanistic comparison. *Curr. Opin. Cell Biol.* 11:68–80.

Fowler, V.M., and E.J.H. Adam. 1992. Spectrin redistributes to the cytosol and is phosphorylated during mitosis in cultured cells. *J. Cell Biol.* 119:1559–1572.

Fujiwara, K., and T.D. Pollard. 1976. Fluorescent antibody localization of myosin in the cytoplasm, cleavage furrow, and mitotic spindle of human cells. *J. Cell Biol.* 71:268–275.

Glotzer, M. 1997. The mechanism and control of cytokinesis. *Curr. Opin. Cell Biol.* 9:815–823.

Glotzer, M., A.W. Murray, and M.W. Kirschner. 1991. Cyclin is degraded by the ubiquitin pathway. *Nature.* 349:132–138.

Gotoh, U., E. Nishida, S. Matsuda, N. Shiina, H. Kosako, K. Shiokawa, T. Akiyama, K. Ohta, and H. Sakai. 1991. In vitro effects on microtubule dynamics of purified *Xenopus* M phase-activated MAP kinase. *Nature.* 349:251–254.

Hamaguchi, Y. 1998. Displacement of cleavage plane in the sea urchin egg by locally applied taxol. *Cell Motil. Cytoskelet.* 40:211–219.

Hara, K. 1971. Cinematographic observation of "surface contraction waves" (SCW) during the early cleavage of axolotl eggs. *Wilhelm Roux's Arch. Dev. Biol.* 186:91–94.

Hara, K., P. Tydeman, and M. Kirschner. 1980. A cytoplasmic clock with the same periodicity as the division cycle in *Xenopus* eggs. *Proc. Natl. Acad. Sci. USA*. 77:462–466.

Hinchcliffe, E.H., G.O. Cassels, C.L. Rieder, and G. Sluder. 1998. The coordination of centrosome reproduction with nuclear events of the cell cycle in the sea urchin zygote. *J. Cell Biol.* 140:1417–1426.

Hiramoto, Y. 1990. Mechanical properties of the dividing sea urchin eggs. *In* Cytokinesis. G.W. Conrad and T.E. Schroeder, editors. *Ann. N.Y. Acad. Sci.* 582:22–30.

Holloway, S.L., M. Glotzer, R.W. King, and A.W. Murray. 1993. Anaphase is initiated by proteolysis rather than by the inactivation of maturation-promoting factor. *Cell.* 73:1393–1402.

Huang, J.Y., and J.W. Raff. 1999. The disappearance of cyclin B at the end of mitosis is regulated spatially in *Drosophila* cells. *EMBO (Eur. Mol. Biol. Organ.) J.* 18:2184–2195.

Ikebe, M., and S. Reardon. 1990. Phosphorylation of bovine platelet myosin by protein kinase C. *Biochemistry.* 29:2713–2720.

Jordan, P., and R. Karess. 1997. Myosin light chain–activating phosphorylation sites are required for oogenesis in *Drosophila. J. Cell Biol.* 139:1805–1819.

Karess, R.E., X.J. Chang, K.A. Edwards, S. Kulkarni, I. Auiera, and D.P. Kiehart. 1991. The regulatory light chain of nonmuscle myosin is encoded by *spaghetti-squash*, a gene required for cytokinesis in *Drosophila. Cell.* 65: 1177–1189.

Kiehart, D.P. 1982. Microinjection of echinoderm eggs: apparatus and procedures. *Methods Cell Biol.* 25:13–31.

Matsumura, F., S. Ono, Y. Yamakita, G. Totsukawa, and S. Yamashiro. 1998. Specific localization of serine 19 phosphorylated myosin II during cell locomotion and mitosis of cultured cells. *J. Cell Biol.* 140:119–129.

McCollum, D., A. Geoktistova, and K.L. Gould. 1999. Phosphorylation of the myosin-II light chain does not regulate the timing of cytokinesis in fission yeast. *J. Biol. Chem*. 274:17691–17695.

McNally, F. 1996. Modulation of microtubule dynamics during the cell cycle. *Curr. Opin. Cell Biol.* 8:23–29.

McNally, F., and S. Thomas. 1998. Katanin is responsible for the M-phase microtubule-severing activity in *Xenopus* egg. *Mol. Biol. Cell.* 9:1847–1861.

McNally, F., and R.D. Vale. 1993. Identification of katanin, an ATPase that severs and disassembles stable microtubules. *Cell.* 75:419–429.

Meijer, L., A. Borgne, O. Mullner, J.P.J. Chang, J.J. Blow, N. Inagaki, M. Inagaki, J.-G. Delcros, and J.P. Moulinoux. 1997. Biochemical and cellular effects of roscovitine, a potent and selective inhibitor of the cylin-dependent kinases cdc2, cdk2 and cdk5. *Eur. J. Biochem*. 243:527–536.

Miller, K.G., and D.P. Kiehart. 1995. Fly division. *J. Cell Biol.* 131:1–5.

Mishima, M., and I. Mabuchi. 1996. Cell cycle-dependent phosphorylation of smooth muscle myosin light chain in sea urchin egg extracts. *J. Biochem*. 119: 906–913.

Murata-Hori, M., N. Murai, S. Komatsu, Y. Uji, and H. Hosoya. 1998. Concentration of a singly phosphorylated myosin II regulatory light chain along the cleavage furrow of dividing HeLa cells. *Biomed. Res.* 19:111–115.

Murray, A.W., M.J. Solomon, and M.W. Kirschner. 1989. The role of cyclin synthesis and degradation in the control of maturation promoting factor activity. *Nature.* 339:280–286.

Neujahr, R., C. Heizer, and G. Gerisch. 1997. Myosin II-independent processes in mitotic cells of *Dictyostelium discoideum*: redistribution of the nuclei, rearrangement of the actin system and formation of the cleavage furrow. *J. Cell Sci.* 110:123–137.

Nishikawa, M.J.R.S., R.S. Adelstein, and H. Hidaka. 1987. Protein kinase C modulates in vitro phosphorylation of the smooth muscle heavy meromyosin by myosin light chain kinase. *J. Biol. Chem*. 259:8808–8814.

Nurse, P. 1990. Universal control mechanism regulating onset of M-phase. *Nature.* 344:503–508.

Ookata, K., S. Hisanaga, J.C. Bulinski, H. Murofuschi, H. Aizawa, T. Itoh, H. Hotani, E. Okumura, K. Tachibana, and T. Kishimoto. 1995. Cyclin B interaction with microtubule-associated protein 4 (MAP4) targets p34cdc2 kinase to microtubules and is a potential regulator of M-phase microtubule dynamics. *J. Cell Biol.* 128:849–862.

Ostrow, B.D., P. Chen, and R.L. Chisholm. 1994. Expression of a myosin regulatory light chain phosphorylation site mutant complements the cytokinesis and developmental defects of *Dictyostelium* RMLC-null cells. *J. Cell Biol.* 127:1945–1955.

Pérez-Mongiovi, D., P. Chang, and E. Houliston. 1998. A propagated wave of MPF activation accompanies surface contraction waves at first mitosis in *Xenopus. J. Cell Sci.* 111:385–393.

Rankin, S., and M.W. Kirschner. 1997. The surface contraction waves of *Xenopus* eggs reflect the metachronous cell-cycle state of the cytoplasm. *Curr. Biol.* 7:451–454.

Rappaport, R. 1961. Experiments concerning the cleavage stimulus in sand dollar eggs. *J. Exp. Zool.* 148:81–89.

Rappaport, R. 1969. Aster-equatorial surface relations and furrow establishment. *J. Exp. Zool.* 171:59–67.

Rappaport, R. 1971. Reversal of chemical cleavage inhibition in echinoderm eggs. *J. Exp. Zool.* 176:249–255.

Rappaport, R. 1975. Establishment and organization of the cleavage mechanism. *In* Molecules and Cell Movement. S. Inoue and R.E. Stephens, editors. Raven Press, New York. 287–304.

Rappaport, R. 1981. Cytokinesis: cleavage furrow establishment in cylindrical sand dollar eggs. *J. Exp. Zool.* 217:365–375.

Rappaport, R. 1985. Repeated furrow formation from a single mitotic apparatus in cylindrical sand dollar eggs. *J. Exp. Zool.* 234:167–171.

Rappaport, R. 1996. Cytokinesis in Animal Cells. Cambridge University Press, Cambridge, UK. 386 pp.

Rappaport, R. 1997. Cleavage furrow establishment by the moving mitotic apparatus. *Dev. Growth Differ.* 39:221–226.

Rappaport, R., and R.P. Ebstein. 1965. Duration of stimulus and latent periods preceding furrow formation in sand dollar eggs. *J. Exp. Zool.* 158:373–382.

Rappaport, R., and B.N. Rappaport. 1984. Division of constricted and urethane-treated sand dollar eggs: a test of the polar stimulation hypothesis. *J. Exp. Zool.* 231:81–92.

Rappaport, R., and B.N. Rappaport. 1987. Relations between interastral distance, time of furrow initiation and the rate of furrow progress in cylindrical sand dollar eggs. *J. Exp. Zool.* 243:417–422.

Rappaport, R., and B.N. Rappaport. 1993. Duration of division-related events in cleaving sand dollar eggs. *Dev. Biol.* 158:265–273.

Rappaport, R., and J.H. Ratner. 1967. Cleavage of sand dollar eggs with altered patterns of new surface formation. *J. Exp. Zool.* 165:89–100.

Rieder, C.L., A. Khodjakov, L.V. Paliulis, T.M. Fortier, R.W. Cole, and G. Sluder. 1997. Mitosis in vertebrate somatic cells with two spindles: implications for the metaphase/anaphase transition checkpoint and cleavage. *Proc. Natl. Acad. Sci. USA.* 94:5107–5112.

Salmon, E.D., and S.M. Wolniak. 1990. Role of microtubules in stimulating cytokinesis in animal cells. *In* Cytokinesis. G.W. Conrad and T.E. Schroeder, editors. *Ann. N.Y. Acad. Sci.* 582:88–98.

Sanger, J.M., J.S. Dome, and J.W. Sanger. 1998. Unusual cleavage furrows in vertebrate tissue culture cells: insights into the mechanisms of cytokinesis. *Cell Motil. Cytoskelet.* 39:95–106.

Satterwhite, L.L., and T.D. Pollard. 1992. Cytokinesis. *Curr. Opin. Cell Biol.* 4:43–52.

Satterwhite, L.L., M.H. Lohka, K.L. Wilson, T.Y. Scherson, L.J. Cisek, J.L. Corden, and T.D. Pollard. 1992. Phosphorylation of myosin-II regulatory light chain by cyclin-p34cdc2: a mechanism for the timing of cytokinesis. *J. Cell Biol.* 118:595–605.

Savoian, M.S., W.C. Earnshaw, A. Khodjakov, and C.L. Rieder. 1999. Cleavage furrows formed between centrosomes lacking an intervening spindle and chromosomes contain microtubule bundles, INCENP, and CHO1 but not CENP-E. *Mol. Biol. Cell.* 10:297–311.

Schroeder, T.E. 1968. Cytokinesis: filaments in the cleavage furrow. *Exp. Cell Res.* 53:272–276.

Schroeder, T.E. 1972. The contractile ring. II. Determining its brief existence, volumetric changes and vital role in cleaving *Arbacia* eggs. *J. Cell Biol.* 53: 419–434.

Sellers, J.R. 1991. Regulation of cytoplasmic and smooth muscle myosin. *Curr. Opin. Cell Biol.* 3:98–104.

Totsukawa, G., E. Himi-Nakamura, S. Komatsu, K. Iwata, A. Tezuka, H. Sakai, K. Yazaki, and H. Hosoya. 1996. Mitosis-specific phosphorylation of smooth muscle regulatory light chain of myosin II at Ser-1 and/or -2 and Thr-9 in sea urchin egg extract. *Cell Struct. Funct.* 21:475–482.

Turbedsky, K., T.D. Pollard, and A.R. Bresnick. 1997. A subset of protein kinase C phosphorylation sites on the myosin II regulatory light chain inhibits phosphorylation by myosin light chain kinase. *Biochemistry.* 36:2063–2067.

Uyeda, T.Q., and J.A. Spudich. 1993. A functional recombinant myosin II lacking a regulatory light chain-binding site. *Science.* 262:1867–1870.

Vandré, D.D., V.E. Centonze, J. Peloquin, R.M. Tombes, and G.G. Borisy. 1991. Proteins of the mammalian mitotic spindle: phosphorylation/dephosphorylation of MAP-4 during mitosis. *J. Cell Sci.* 98:577–588.

Verde, F., L.C. Labbe, M. Doree, and E. Karsenti. 1990. Regulation of microtubule dynamics by cdc2 protein kinase in cell-free extracts of *Xenopus* eggs. *Nature.* 343:233–238.

Walczak, C.E., T.J. Mitchison, and A. Desai. 1996. XKCM1: a *Xenopus* kinesin-related protein that regulates microtubule dynamics during mitotic spindle assembly. *Cell.* 84:37–47.

Walker, G., D. Burgess, and W.H. Kinsey. 1996. Fertilization promotes selective association of the Abl kinase with the egg cytoskeleton. *Eur. J. Cell Biol.* 70:165–171.

Walker, G.R., R. Kane, and D.R. Burgess. 1994. Isolation and characterization of a sea urchin zygote cortex that supports in vitro contraction and reactivation of furrowing. *J. Cell Sci.* 107:2239–2248.

Walker, G.R., C.B. Shuster, and D.R. Burgess. 1997. Microtubule-entrained kinase activities associated with the cortical cytoskeleton during cytokinesis. *J. Cell Sci.* 110:1373–1386.

Wheatley, S.P., and Y.L. Wang. 1996. Midzone microtubule bundles are continuously required for cytokinesis in cultured epithelial cells. *J. Cell Biol.* 135: 981–989.

Wheatley, S.P., E.H. Hinchcliffe, M. Glotzer, A.A. Hyman, G. Sluder, and Y.L. Wang. 1997. CDK1 inactivation regulated anaphase spindle dynamics and cytokinesis in vivo. *J. Cell Biol.* 138:385–393.

Yabkowitz, R., and D.R. Burgess. 1987. Low ionic strength solubility of myosin in sea urchin egg extracts is mediated by a myosin-binding protein. *J. Cell Biol.* 105:927–936.

Yamakita, Y., S. Yamashiro, and F. Matsumura. 1994. In vivo phosphorylation of regulatory light chain of myosin II during mitosis of cultured cells. *J. Cell Biol.* 124:129–137.

Yamashiro, S., Y. Yamakita, H. Hosoya, and F. Matsumura. 1991. Phosphorylation of non-muscle caldesmon by p34cdc2 kinase during mitosis. *Nature.* 349:169–172.

Zang, J.H., G. Cavet, J.H. Sabry, P. Wagner, S.L. Moores, and J.A. Spudich. 1997. On the role of myosin-II in cytokinesis: division of *Dictyostelium* cells under adhesive and nonadhesive conditions. *Mol. Biol. Cell.* 8:2617–2629.